Estimates of future discharges of the river Rhine using two scenario methodologies: direct versus delta approach

G. Lenderink, A. Buishand, W. van Deursen

Hydrol. Earth Syst. Sci., 11(3), 1145–1159, 2007
www.hydrol-earth-syst-sci.net/11/1145/2007

Hydrology & Earth System Sciences

Estimates of future discharges of the river Rhine using two scenario methodologies: direct versus delta approach

Geert Lenderink[1], Adri Buishand[1] and Willem van Deursen[2]

[1]KNMI (Royal Netherlands Meteorological Institute), De Bilt, The Netherlands
[2]Carthago Consultancy, Rotterdam, The Netherlands

Email for corresponding author: lenderin@knmi.nl

Abstract

Simulations with a hydrological model for the river Rhine for the present (1960–1989) and a projected future (2070–2099) climate are discussed. The hydrological model (RhineFlow) is driven by meteorological data from a 90-years (ensemble of three 30-years) simulation with the HadRM3H regional climate model for both present-day and future climate (A2 emission scenario). Simulation of present-day discharges is realistic provided that (1) the HadRM3H temperature and precipitation are corrected for biases, and (2) the potential evapotranspiration is derived from temperature only. Different methods are used to simulate discharges for the future climate: one is based on the direct model output of the future climate run (direct approach), while the other is based on perturbation of the present-day HadRM3H time series (delta approach). Both methods predict a similar response in the mean annual discharge, an increase of 30% in winter and a decrease of 40% in summer. However, predictions of extreme flows differ significantly, with increases of 10% in flows with a return period of 100 years in the direct approach and approximately 30% in the delta approach. A bootstrap method is used to estimate the uncertainties related to the sample size (number of years simulated) in predicting changes in extreme flows.

Keywords: climate change impact, regional climate model, extreme river flows

Introduction

The Rhine is the longest river in Western Europe. Its basin of 185 000 km^2 extends from the Swiss Alps to Germany, France and, finally, to the Dutch coast where the river discharges into the North Sea (Fig. 1). The Rhine has a large influence on water resources, is used widely for navigation and bears a potential risk of flooding to large areas. It is, therefore, important to estimate and to understand potential changes in its discharge in a changing climate (Kwadijk and Rotmans 1995; Middelkoop 2000; Shabalova *et al.* 2003).

To estimate the impact of climate change on river discharges, different scenarios of future meteorological conditions (mainly temperature, precipitation and evapotranspiration) are used as input to a hydrological model of the river basin; the outputs are the corresponding discharges. These climate scenarios are usually constructed by applying simple transformation rules to observed temperature and precipitation (e.g. Snover *et al*., 2003). This method is referred to as the delta change approach (Hay *et al.,* 2000) or delta (forcing) approach. A simple, commonly used, delta approach for temperature adds an 'expected' temperature increase to the observed temperature record to obtain a future temperature time series. Precipitation is usually perturbed by a fraction. These rules imply that only simple changes in the probability density function of these variables are taken into account; thus, the variance of temperature and the coefficient of variation (CV) of precipitation are unchanged. Furthermore, changes in the number of days of precipitation and potential changes in the correlation between the different variables are not considered.

Recently, high-resolution Regional Climate Models (RCMs) have been developed (Jones *et al.*, 2001; Vidale *et al*., 2003; Jones *et al*., 2004; Giorgi *et al*., 2004; Räisänen *et al.,* 2004) within co-operative projects such as

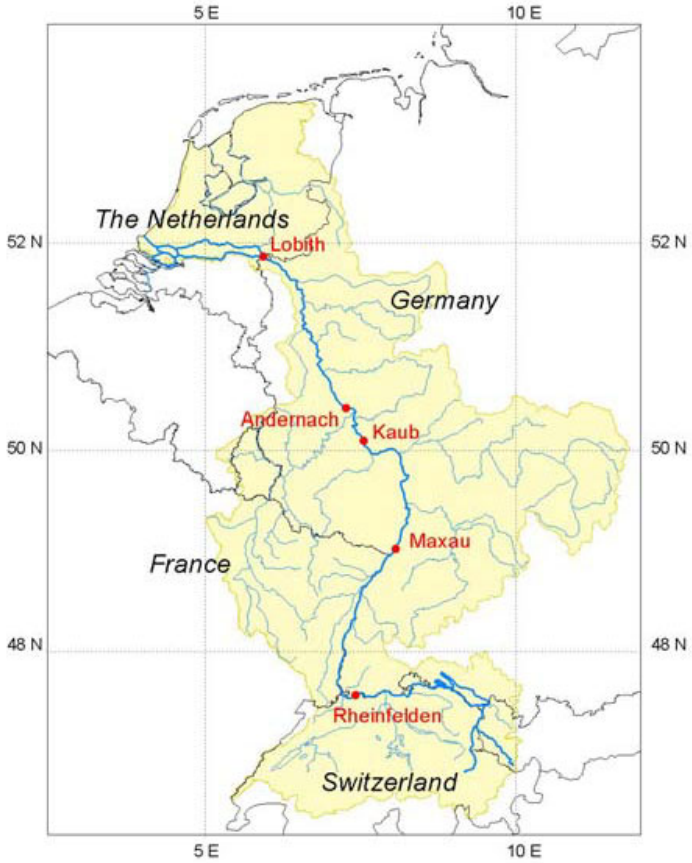

Fig. 1. *Basin of the river Rhine, with the locations of five gauging stations.*

PRUDENCE (Prediction of Regional scenarios and Uncertainties for Defining EuropeaN Climate change risks and Effects) (Christensen and Christensen, 2002) and in regional model intercomparison projects like PIRCS (Project to Intercompare Regional Climate Simulations, Tackle *et al.,* 1999). Increases in computer power have led to RCMs with typical resolutions of about 50 km and resolutions of 10 km are foreseeable. This development enables changes in river discharges to be estimated using the output of the RCMs 'directly' (because some corrections must be made to the RCM output) to force the hydrological model (Hay *et al.,* 2002; Graham, 2004). This direct forcing approach has the potential advantage of taking into account more complex changes in the probability density functions of the input variables of the hydrological models. Correlations between the different climatic variables may change in the regional climate simulations, which might affect the output of the hydrological model. However, these potential advantages might (easily) become a disadvantage if the quality of the RCM output is not good enough. This rather vague phrase has been used because not much is known about how to quantify 'good' in relation to the application of regional model outputs in hydrological models. The first part of this paper focuses on this aspect: how must the direct output of the regional climate model be corrected to obtain realistic discharges in the present climate?

The second part of the paper deals with the change in the discharges between the control period (1960–1989) and a future period (2070–2099). The future scenario uses the SRES A2 greenhouse gas emission scenario of the Intergovernmental Panel on Climate Change IPCC (Nakicenovic *et al.,* 2000). Changes in the mean discharge and in extreme flows are discussed. The results obtained by direct forcing have been compared with those by a delta approach; this estimates the influence of the method of scenario production on the changes predicted in river flow characteristics. In particular, since society demands estimates of discharges occurring once every 100–1000 years, changes in such discharges have been estimated by fitting a Gumbel distribution to the annual maximum discharges. It is generally accepted that the limited number of years simulated (typically 30 years) means that the level of confidence in predicting changes in extremes with a return period of more than one year is low (Frei and Schär, 2001; Klein Tank and Können, 2003). Therefore, the uncertainty related to the sample size is estimated using the bootstrap.

The output of the UK Met Office regional climate model HadRM3H has been fed into the hydrological model, RhineFlow, to estimate the 10-day discharges of the river Rhine at Lobith at the German–Netherlands border (Fig. 1).

Models

RHINEFLOW

The RhineFlow hydrological model is a spatially distributed water balance model of the Rhine basin that simulates river flow, soil moisture, snow pack and groundwater storage with a 10-day time step. The model describes three types of runoff: direct runoff at the surface, rapid runoff from a relatively thin active soil layer, and delayed runoff from a deep groundwater reservoir. The model operates on a grid of 3 × 3 km^2. Although the Rhine is a highly utilised river, much of the river system is still without major control structures. Some adjustments, however, are made for the regulations of lakes in the Swiss Alps (Kwadijk and Rotmans, 1995). The time step of 10 days is sufficiently long to avoid explicit hydraulic routing, which is supported by observations of travel time through the main branch of the Rhine in the order of 3 to 6 days (CHR, 1976). The model used here is an updated version of the model used by Shabalova *et al.* (2003), which has been recalibrated to improve the simulation of low flows using discharges observed at five gauging stations along the Rhine (Fig. 1) over the period 1961–1974. A full description of the RhineFlow model is given in van Deursen and Kwadijk (1993), and Kwadijk and Rotmans (1995).

Apart from geographical information on topography, land use, soil type and groundwater flow characteristics, the following meteorological input variables are used: 10-day averages of daily maximum, minimum and mean temperature, potential evapotranspiration (PET) and precipitation. The minimum and maximum temperatures are used in the calculation of snow accumulation and snow melt. Potential evapotranspiration is represented as the product of a crop factor and reference evapotranspiration, as provided by the different meteorological services. The conversion of potential to actual evapotranspiration is based on Thornthwaite and Mather (1957). For the 35-year period, precipitation data were available for about 200 sub-catchments in Germany, over 30 stations in France and for a 2 × 2 km^2 grid in Switzerland. Temperatures and an estimate of potential evapotranspiration were obtained for more than 70 stations in the Rhine basin.

The results of RhineFlow, driven by observations of temperature and precipitation and by values of potential evapotranspiration calculated from the observations, are shown in Fig. 2. The time series of the maximum discharge

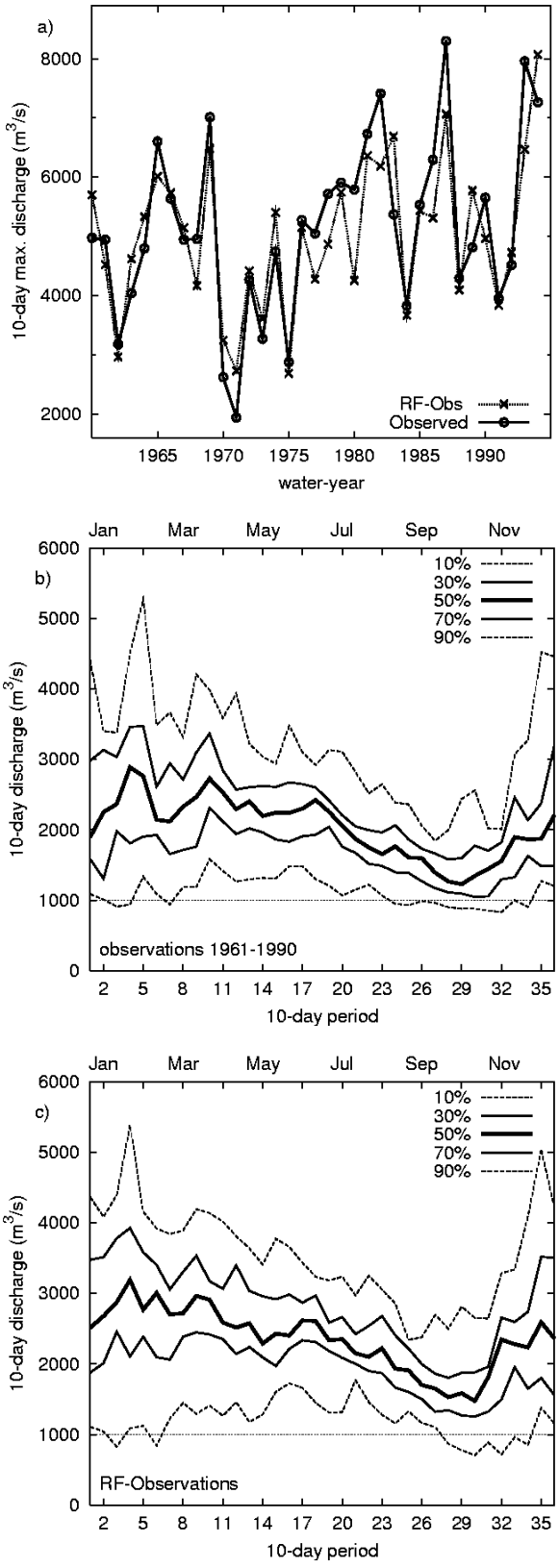

Fig. 2: (a) Time series of the maximum discharge in a water-year at Lobith as simulated by RhineFlow driven by observed meteorological data. Quantiles of observed (b) and simulated (c) 10-day discharges as a function of time of the year.

in the water-year (from 1 October of the previous year to 30 September of the present year) shows a good correspondence between the RhineFlow simulation and the observations at Lobith. For the maximum discharge the correlation between the model output and observations is 0.87; the mean difference is –120 $m^3 s^{-1}$, and the RMS difference is 730 $m^3 s^{-1}$. The lower panels compare the quantiles of modelled and observed 10-day discharges. In winter and early spring, the range between the 10% and 90% quantile is between 1000 and 4000 $m^3 s^{-1}$ for both the observations and the model run. Discharges and interquantile ranges for both model and observations are minimal in September and October while the median (50% quantile) decreases gradually from 3000 $m^3 s^{-1}$ in January to nearly 1500 $m^3 s^{-1}$ in September and October, followed by a rapid recovery to winter values in late autumn and early winter.

HADRM3H

The meteorological data are derived from output of the regional climate model HadRM3H, which is the third generation limited area model of the UK Met Office (Jones *et al.,* 2001). It runs on a resolution of about 50 km grid spacing covering an area of roughly 5000 × 5000 km^2. The lateral boundaries are given by the output of a high-resolution global atmospheric model HadAM3H, which uses sea-surface temperatures derived from the output of a global climate model HadCM3 (Johns *et al.*, 2003). More details about the model, model set-up and model performance are given in Ekström *et al*. (2007).

With the regional model, two 30-year periods are considered: the period 1960 to 1989 represents the control climate and that from 2070 to 2099 (A2 emission scenario) the future climate. Three realisations are available for both the control period (denoted C_i, C_j, and C_k) and the future period (denoted F_a, F_b, and F_c). The regional model produces temperature and precipitation as direct outputs. estimates Potential evapotranspiration is derived from a Penman-Monteith equation which considers surface radiation and the saturation deficit between the surface and the atmosphere (Ekström *et al.*, 2007); it is computed from daily data and then averaged to a 10-day period.

To illustrate the performance of HadRM3H for the present climate, values of the mean temperature and precipitation bias are plotted in Fig. 3. Both winter (DJF) and summer (JJA) temperatures show a warm bias of approximately 1K with a rather uniform spatial distribution. The south-eastern part of the domain is too cold in winter. The precipitation bias has a much stronger regional pattern, with large variations at the grid-box scale. In winter, grid boxes with large positive biases (+100%) are located next to grid boxes with large negative biases (–50%). These patterns appear to be related to the topography, with a tendency to high precipitation over the peaks and low precipitation in the valleys (Frei *et al.,* 2003). In summer, the grid-box variations are less pronounced but still visible.

The Rhine area-mean temperature, precipitation and potential evapotranspiration as a function of time of the year (all averaged over 90 years of model output and 30 years of observations) are shown in Fig. 4. The modelled seasonal cycle of the temperature is close to that observed, with a small (1K) bias in summer and winter, but almost none in spring and autumn. The precipitation bias is small in summer and positive for the rest of the year, with typical values between 0.5 and 1.5 mm day^{-1}. Potential evapotranspiration is underestimated in spring and early summer and overestimated in the other seasons. Precipitation in the future climate increases in winter and decreases in summer, while potential evapotranspiration increases over the whole year, with large absolute increases in (late) summer.

Discharges from the control simulation

Here, discharges at Lobith are compared with the direct model output of HadRM3H with various forms of (bias) corrections to the data. The bias in precipitation, of the order of 1 mm day^{-1}, translated directly into run-off, would represent a discharge of about 1800 $m^3 s^{-1}$ at Lobith; hence, a bias correction, in precipitation at least, is essential.

METHOD OF BIAS CORRECTION

For each grid box, the simulated 10-day average precipitation in the control simulation $P_{cont}(t)$ was scaled by the ratio between the long-term means $\overline{P}_{obs}$ and $\overline{P}_{cont}$ of the observed and simulated precipitation amounts for each 10-day time step:

$$P_{cont,cor}(t) = P_{cont}(t) \times (\overline{P}_{obs} / \overline{P}_{cont}), \quad t = 1,\ldots,36J \qquad (1)$$

where J is the number of years ($J = 30$ for a single ensemble member and $J = 90$ for the concatenation of the three ensemble members). The means $\overline{P}_{obs}$ and $\overline{P}_{cont}$ were first calculated for each of the 36 periods of 10 days in the year and then smoothed using a Gaussian filter of seven 10-day periods to reduce the effect of sampling variability. The bias correction is the same for the three ensemble members ($\overline{P}_{cont}$ is the average value of these members C_i, C_j and C_k) and, thus, the differences between the three ensemble members are retained.

The bias in potential evapotranspiration is corrected in

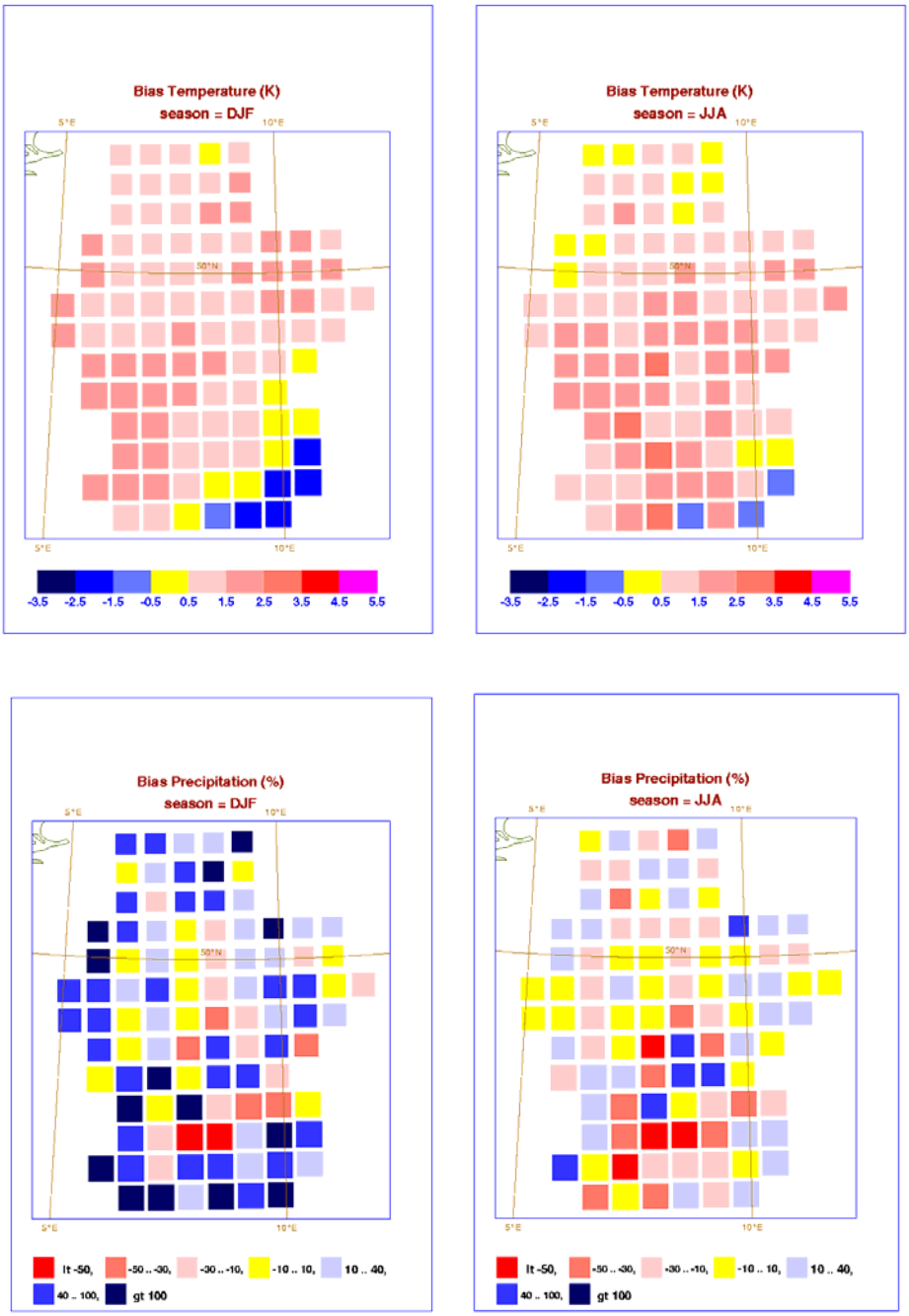

Fig. 3. Bias of the HadRM3H simulation in mean winter (DJF) and summer (JJA) temperature (in K), and precipitation (in %).

the same way as that in precipitation. Finally, for the mean temperature, addition was used rather than multiplication, so that:

$$T_{\mathrm{cont,cor}}(t) = T_{\mathrm{cont}}(t) + (\overline{T}_{\mathrm{obs}} - \overline{T}_{\mathrm{cont}}), \quad t = 1,\ldots,36J \quad (2)$$

Correcting the minimum and maximum temperature with the same quantity ensures that the minimum temperature never exceeds the mean temperature; likewise the maximum is never lower than the mean; this procedure leaves the diurnal temperature range in the original HadRM3H data set unaffected (and uncorrected).

After correction, the bias in the area-mean, 30 years' averaged temperature and potential evapotranspiration is insignificant but, for precipitation, significant bias remains for some 10-day periods as shown in Fig. 4. This is due to

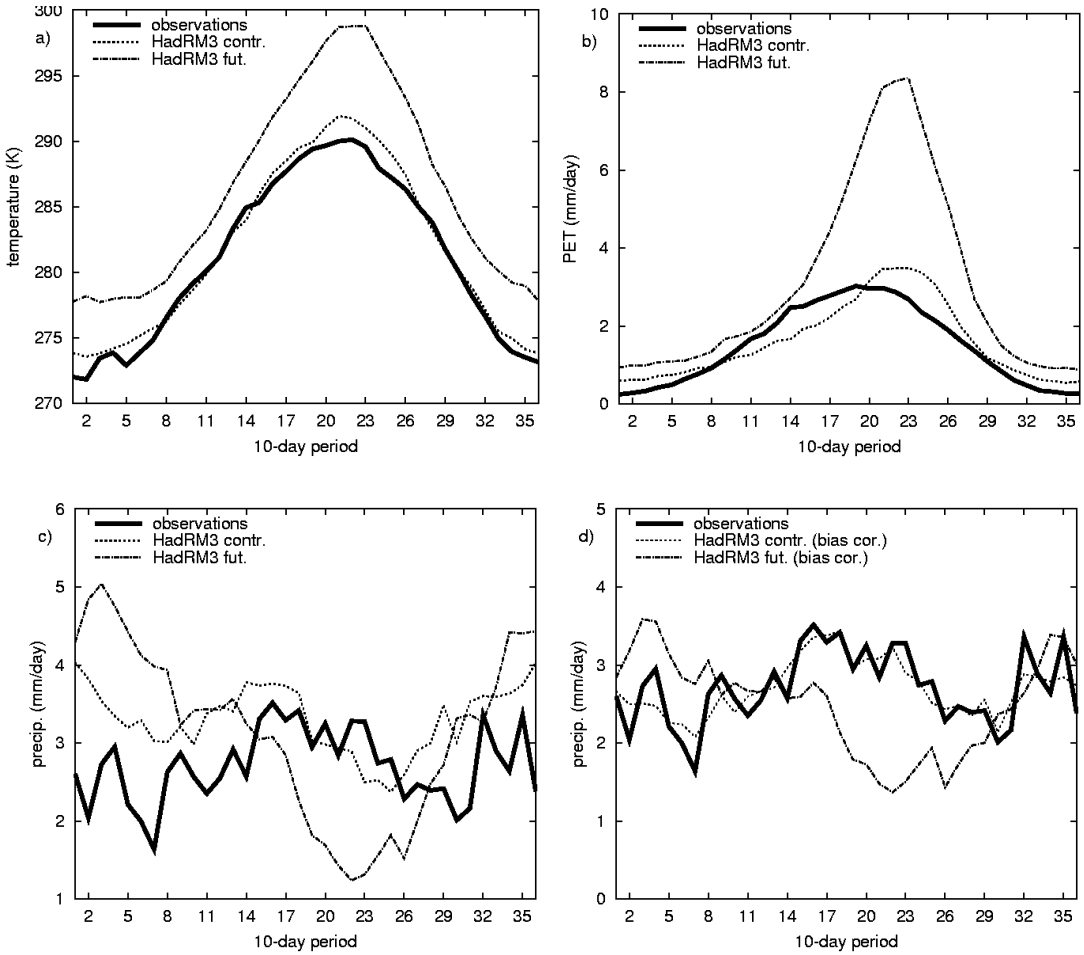

Fig. 4. *Area-mean (a) temperature, (b) PET, (c) precipitation, and (d) precipitation after bias correction, as a function of 10-day period. Shown are observations averaged over 1961 to 1990, and the HadRM3H control and future simulation (averaged over 90 years).*

the Gaussian filtering. On a seasonal mean basis, the bias is nevertheless small with values less than 0.02 mm day^{-1}. The 10-day, basin-mean precipitation exceedance probabilities for the summer and winter months after bias correction are plotted in Fig. 5; occurrences of 10-day, basin-mean precipitation amounts of more than 5 mm day^{-1} are seen to be overestimated in summer and underestimated in winter.

DISCHARGES

Results from the RhineFlow model simulations driven with and without bias corrections (Fig. 6) are compared with the model output of RhineFlow driven by observations, rather than observed discharges directly. This attempts to separate the errors in the RhineFlow model from those introduced by the meteorological input given by the HadRM3H data.

It is not surprising that running RhineFlow directly, without any correction, with HadRM3H data, does not give realistic discharge data. Using output of the uncorrected control climate run C_i yields an average discharge as high as 4000 m^3 s^{-1} in winter and early summer (Fig. 6). After bias correction of the precipitation, the annual mean discharge shows a large improvement. However, the annual cycle is still incorrect with the peak discharge in summer and relatively low discharges in winter. Qualitatively, the seasonal course of the bias in potential evapotranspiration is consistent with the bias in discharge. In winter, the potential evapotranspiration is over-estimated whereas in spring and early summer it is under-estimated.

After corrections of potential evapotranspiration and temperature, the response of RhineFlow gives more realistic values of discharge in winter but, although there is an improvement in the summer response, the mean discharge in July and August remains too high (Fig. 6 left panel on top).

Notwithstanding the correction for bias of all the input variables which, therefore, represent a realistic time mean forcing, the response of the hydrological model does not

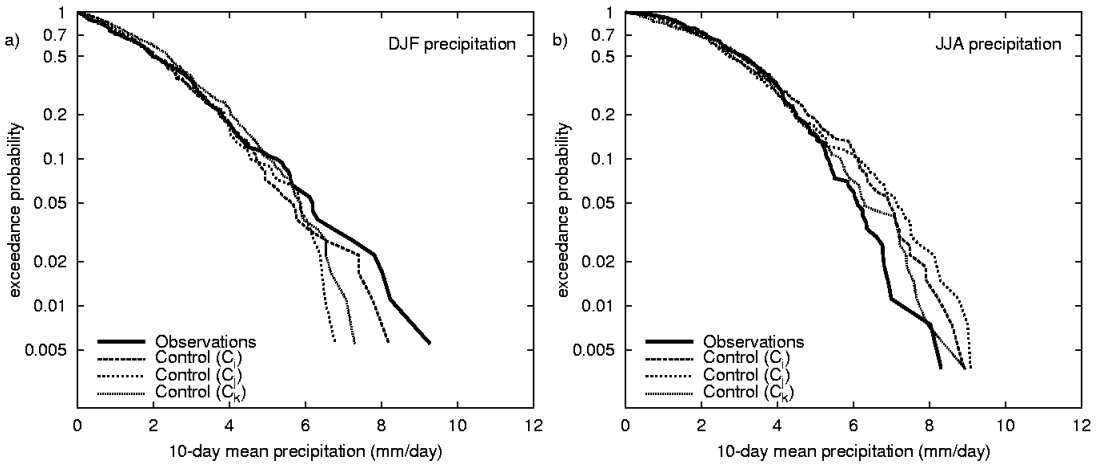

Fig. 5. *Exceedance probabilities of 10-day basin-mean precipitation for the three ensemble members (after bias correction) for the control simulation compared to observations.*

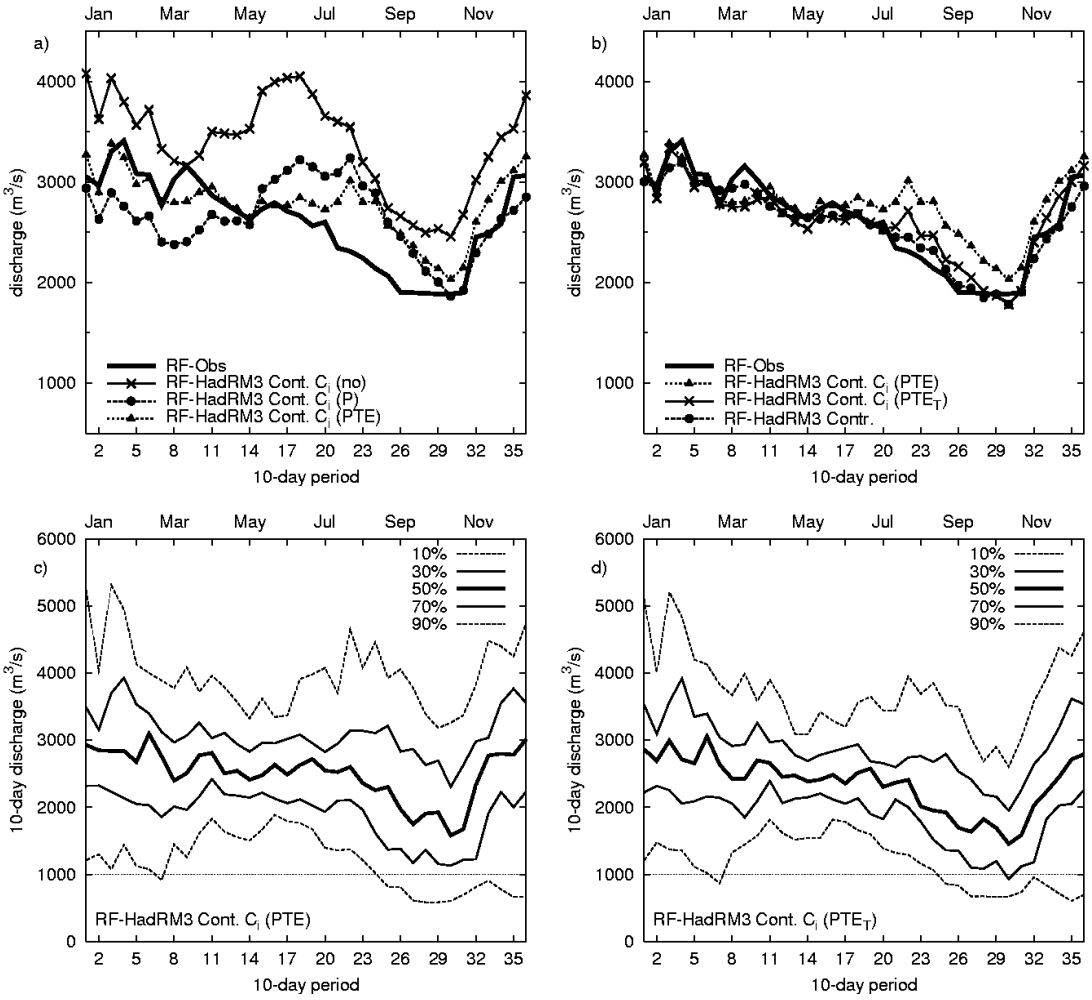

Fig. 6. *Mean and quantiles of the 10-day discharge as a function of time of the year in different RhineFlow (RF) simulations. The following notations are used: Obs denotes the RhineFlow simulation driven by observations, and HadRM3H Cont. C_i a RhineFlow simulation driven by ensemble member C_i (30 years), with in parentheses the level of bias-correction: 'no' denotes uncorrected data; P denotes bias corrected precipitation (and otherwise uncorrected), PTE denotes bias corrected Precipitation, Temperature and potential Evapotranspiration; E_T denotes the temperature based reconstruction of potential evapotranspiration. HadRM3H Contr. (with no further specification) denotes the 90 years corrected PTE_T simulation (standard control simulation).*

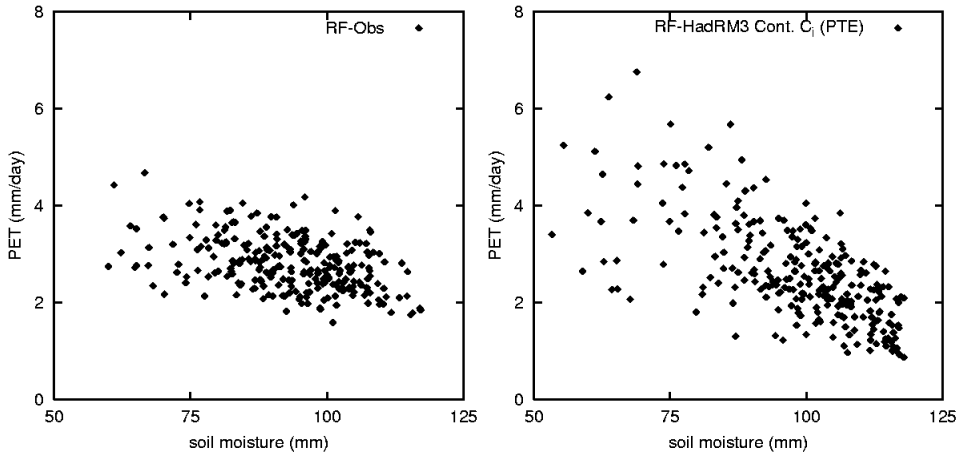

Fig. 7. *Scatter plots of PET against available soil moisture for evapotranspiration in RhineFlow for the simulation driven by observations (left-hand panel) and the simulation driven by HadRM3H run C_i (with bias corrections). Shown are the basin-mean values for all 10-day periods in JJA.*

give the correct mean discharge. This is related to the conversion from potential to actual evapotranspiration, which is a function of the potential evapotranspiration as given by the meteorological forcing data and the soil moisture content as given by the hydrological model:

$$E = f(w_s, PET) \tag{3}$$

In RhineFlow, the actual evapotranspiration is the product of normalised soil moisture w_s (as a fraction of the water holding capacity) and potential evapotranspiration. Therefore, to achieve a realistic mean actual evapotranspiration, the relation between soil moisture and potential evapotranspiration must be realistic. This is not entirely trivial. Figure 7 shows, for the summer months, a scatter plot of potential evapotranspiration (used to force the hydrological model) against soil moisture (from the hydrological model). In the run driven by observations, there is only a weak correlation (correlation coefficient –0.42) between soil moisture and PET (left-hand side of Fig. 7). However, in the run driven by HadRM3H data (ensemble member C_i), there is a clear relationship between these two quantities with a correlation coefficient of –0.73 (right-hand side of Fig. 7). The range in 10-day mean potential evapotranspiration is much larger in HadRM3H (between 1 and 9 mm day^{-1}) than in the observations (between 2 and 4 mm day^{-1}). Together with the high correlation between soil moisture and PET in the HadRM3H driven simulation, this implies a lower value of the mean actual evapotranspiration.

Focusing more on the forcing meteorological data, Fig. 8 is a scatter plot of monthly means of potential evapotranspiration against temperature for both observations and bias-corrected HadRM3H data (runs C_i, C_j and C_k). The

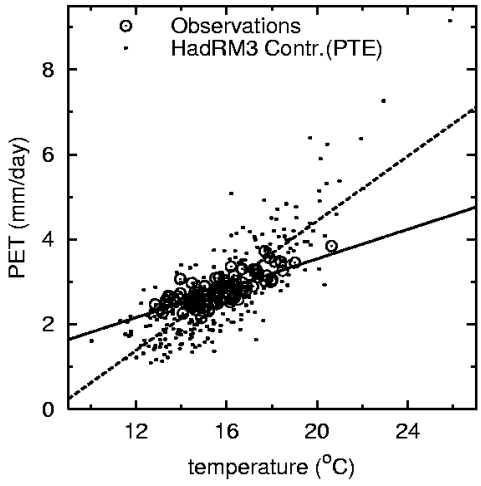

Fig. 8. *Scatter plot of PET against monthly mean temperature in the observations and in HadRM3H (bias corrected). The solid line denotes a fit through the observations, and the dashed line a fit through the model data.*

temperature dependency of the potential evapotranspiration is about twice as strong in HadRM3H as in the observations. Hence, potential evapotranspiration was recalculated from temperature only using a simple linear regression, expressing potential evapotranspiration anomalies in terms of temperature anomalies as in Ekström *et al.* (2007). With the re-computed potential evapotranspiration, which has by construction no bias in the means, the mean discharge in summer decreased by approximately 500 m^3 s^{-1}. In summer, the spread (Fig. 6c, d) also decreased, although the variability was still larger than that observed (Fig.2 b). A factor that contributes to this spread is the over-estimation of high precipitation amounts in summer by the HadRM3H simulations as shown in Fig. 5. Changing from the one-

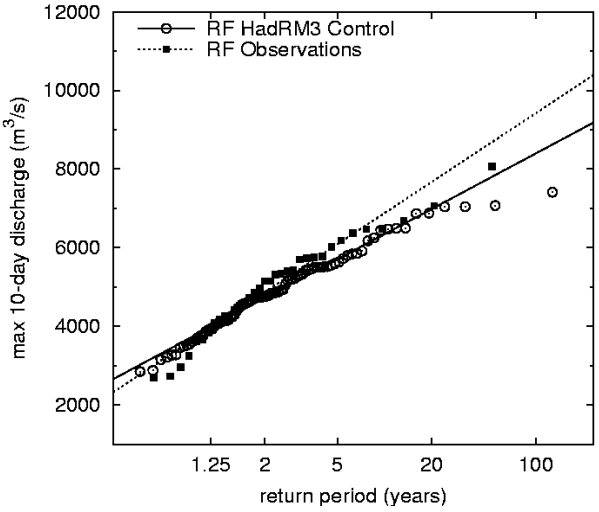

Fig. 9. *Gumbel plot of the maximum discharges as simulated by RhineFlow driven by observations and RhineFlow driven by the HadRM3 control simulation. The lines are based on maximum likelihood fits.*

ensemble member integrations (30 years) to the three-ensemble members (90 years) has only a marginal effect on the mean discharge (Fig. 6, right panel on top), as well as on the quantiles.

Finally, the ability to reproduce the distribution of extreme runoff events using HadRM3H data was investigated. Following Shabalova *et al.* (2003) a Gumbel distribution was fitted to the annual maximum, 10-day average, discharges $Q_{\max}$ in the water-year (from October to September). The Gumbel distribution is given by:

$$F(x) = \Pr(Q_{\max} \le x) = \exp\left[-\exp\left(-\frac{x-\xi}{\alpha}\right)\right], \quad (3)$$

where ξ is a location parameter and α is a scale parameter. Most annual maximum flows occur in winter. Figure 9 shows a Gumbel plot of annual maximum discharges $Q_{\max}$. The straight lines are maximum likelihood fits to the data. Discharges below 4000 $m^3 s^{-1}$ are censored because of departures from the assumed Gumbel distribution at low return periods, in particular, for the reference simulation driven by observations. The results of the HadRM3H control simulation are reasonably close to the RhineFlow reference simulation. The estimated discharge for a return period of 100 years is 800 $m^3 s^{-1}$ lower in the HadRM3H control simulation.

Future discharges

METHODS

In the delta approach, the baseline control climate time series are perturbed with estimated (mean) climate changes from the regional model simulations. This is scenario 1. The future time series are given by:

$$T_{\text{scen,delta}}(t) = T_{\text{cont,cor}}(t) + (\overline{T}_{\text{fut}} - \overline{T}_{\text{cont}}), \quad t = 1,\ldots,36J \quad (4a)$$

$$P_{\text{scen,delta}}(t) = P_{\text{cont,cor}}(t) \times (\overline{P}_{\text{fut}} / \overline{P}_{\text{cont}}), \quad t = 1,\ldots,36J \quad (4b)$$

Note that the bias-corrected control simulation is used as the reference climate, in contrast with the traditional application of the delta approach where observations are used as a baseline. There are two reasons for this approach. Firstly, the use of 90 years of control simulations (instead of 35 years of observations) increases the accuracy of the estimated changes in the extremes considerably. Secondly, by sharing the same meteorological conditions as for the control climate, the inter-comparison between the two methods is as objective as possible. A drawback is that, with the present version of the delta approach, the excessive hydrological feedback found in the control simulation is carried over to the future climate.

The direct forcing approach, scenario 2, uses the meteorogical data of three HadRM3H ensemble members (denoted by F_a, F_b, and F_c), corrected using the bias of the control simulations. So the future scenario based on the direct forcing approach becomes:

$$T_{\text{scen,direct}}(t) = T_{\text{fut}}(t) + (\overline{T}_{\text{obs}} - \overline{T}_{\text{cont}}), \quad t = 1,\ldots,36J \quad (5a)$$

$$P_{\text{scen,direct}}(t) = P_{\text{fut}}(t) \times (\overline{P}_{\text{obs}} / \overline{P}_{\text{cont}}), \quad t = 1,\ldots,36J \quad (5b)$$

The relative changes for precipitation and potential

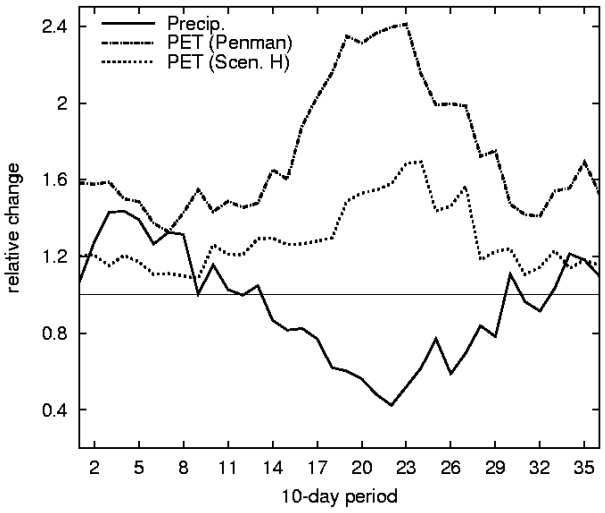

Fig. 10. *Fractional change in basin-mean, 10-day precipitation and PET, computed from the Penman-Monteith equation and using the temperature regression (scenario).*

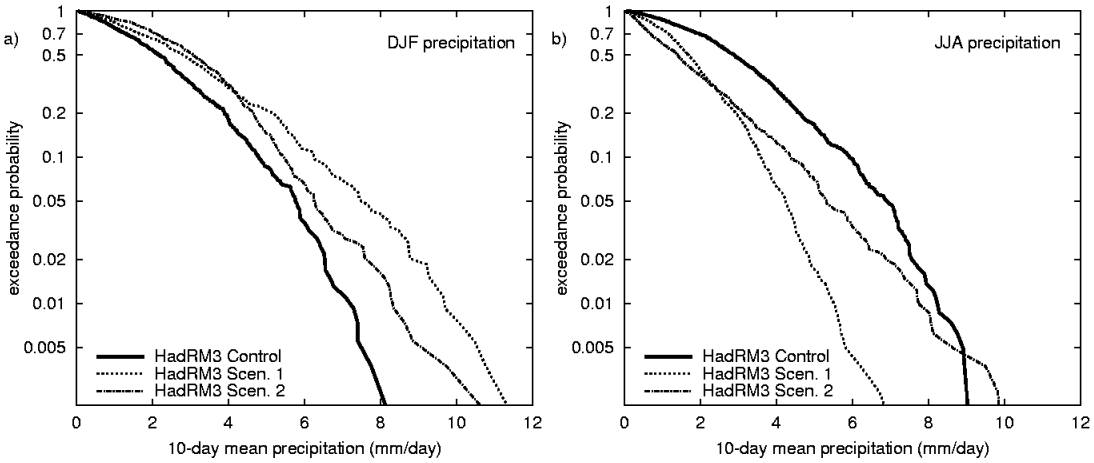

Fig. 11. *Exceedance probabilities of basin-mean 10-day precipitation for the control simulation and the two future scenarios in both winter (DJF) and summer (JJA).*

evapotranspiration are plotted in Fig. 10. For PET, both the value computed from the Penman-Monteith equation and from the temperature regression are plotted. The temperature rise, ranging from 4 degrees in winter to 7 degrees in late summer, can be estimated from Fig. 4.

Brandsma (1995) argued that the dependency of PET on temperature in the present-day climate is not necessarily a good predictor of the sensitivity of PET to climate change. Because the change in PET is highly uncertain, an ensemble of three different evapotranspiration scenarios was used to span a wide range of possible outcomes: *H* assuming that the temperature regression remains valid in the future climate, *M* assuming that the change in mean PET equals half that of scenario *H*, and *L* assuming no change in mean PET (Ekström *et al.* 2007). Method *M* yields values (half the change plotted in Fig. 10) close to those used in previous studies with RhineFlow (Shabalova *et al*. 2003) and is, therefore, used as a reference.

Exceedance probabilities of the 10-day, area-averaged precipitation in the control simulation and in the two future scenarios (direct and delta approach) are shown in Fig. 11. The two scenarios differ considerably, with, in winter, a higher probability of extreme 10-day precipitation in the delta approach while, in summer, the direct approach predicts much more extreme precipitation events.

MEAN FLOW

The mean discharges for the direct and delta approach, all averaged over 90 years, are plotted in Fig. 12. In winter, the increase in mean discharge is about 30%, from 3000 to about 4000 $m^3 s^{-1}$, in response to the increase in precipitation of about 1 mm day^{-1} (corresponding to a discharge of about 1800 $m^3 s^{-1}$); this is moderated by the drier condition of the soil in early winter because of the lower precipitation in summer and autumn and the higher PET. Also, more of the winter precipitation falls as rain and contributes directly to the runoff. In summer, the response is large with decreases in the mean flow of about 40%, yielding a mean discharge of 1000 $m^3 s^{-1}$ or less, reflecting the lower rainfall and the higher values for PET. In early summer, a reduction in snowmelt also contributes to the decrease in discharge (Shabalova *et al.,* 2003).

In winter, both HadRM3H-based scenarios predict almost identical mean discharges but, in summer, the direct forcing approach yields discharges a few hundred $m^3 s^{-1}$ higher. Although the mean discharge in winter is very similar for both scenarios, the variability is different. The spread in the discharge is larger in the delta approach, with a difference of about 4000 $m^3 s^{-1}$ in February between the 90% and the 10% quantiles compared to 3000 $m^3 s^{-1}$ in the direct forcing approach (Fig. 12). In summer, the situation is reversed, with more variability in the direct forcing approach. These results agree with the differences in large precipitation amounts between the two scenarios (Fig. 11).

EXTREMES

To quantify the differences in extreme discharges between the two scenarios, Fig. 13 is a Gumbel plot of annual maximum discharges Q_{max}. The straight lines are maximum likelihood fits to the data, censored from below at 4000 $m^3 s^{-1}$. Using the delta approach, a large increase in extreme discharges is obtained. Extrapolation of the fitted Gumbel distribution to a return period of 100 years results in an increase of 30% over the control simulation; that is, from 8400 $m^3 s^{-1}$ in the control to 11 200 $m^3 s^{-1}$ in the scenario simulation. In contrast, the direct approach results in an

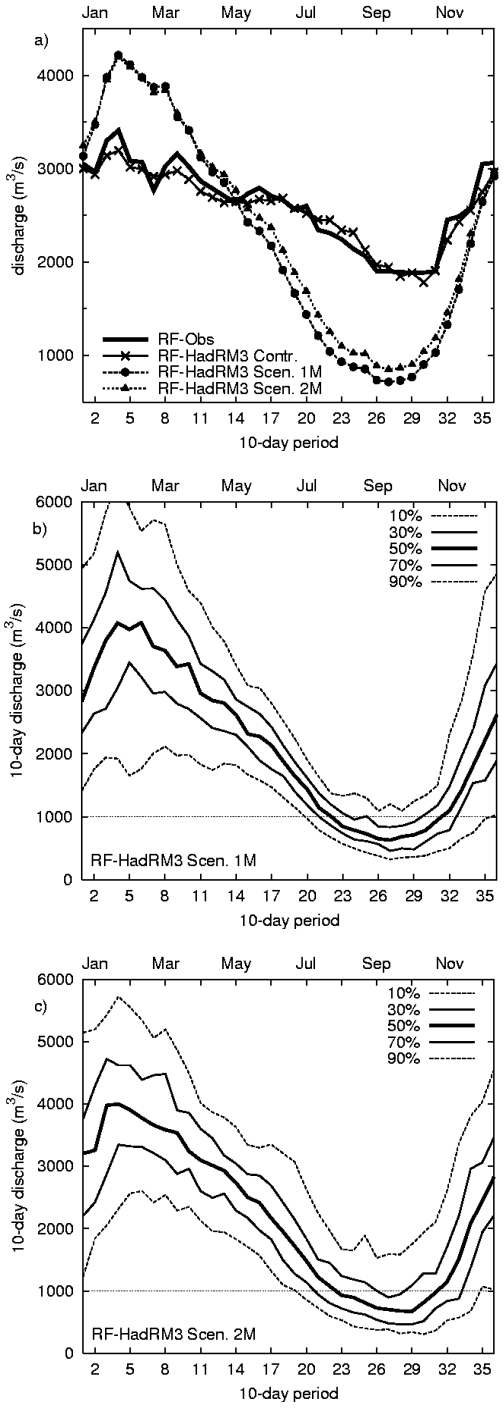

Fig. 12. *Mean discharge and quantiles at Lobith for the different future scenarios.*

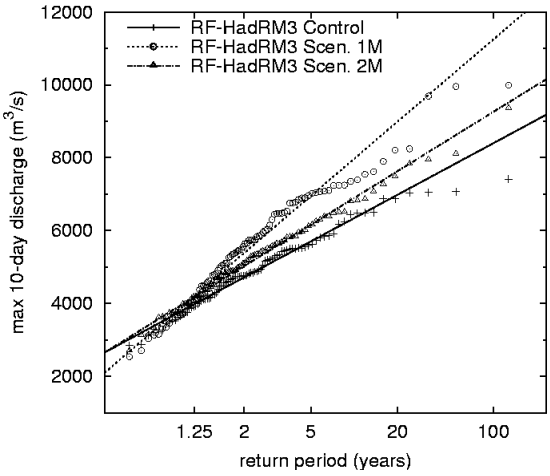

Fig. 13. *Gumbel plot of the annual maximum, 10-day average discharges at Lobith as simulated by RhineFlow for the control simulation and the future scenario runs. The lines are based on maximum likelihood fits. Shown are the results of the delta approach (scenario 1M) and the direct approach (scenario 2M).*

increase of about 10% (to 9300 $m^3 s^{-1}$). Note that for the delta approach the simulated extremes with return periods of 5 years or more seem to fall consistently below the fitted line, in part because of the property of RhineFlow to underestimate extreme flows. In addition, in the control simulation the highest extreme discharge events already fall consistently below the Gumbel fit, which may well reflect the under-estimation in all ensemble members of extreme 10-day precipitation events in winter with 5 mm day^{-1} or more over the basin. Since the delta approach simply scales the precipitation using Eqn. (4b), this characteristic could easily carry over to the results of the future scenario run.

SENSITIVITY TO EVAPOTRANSPIRATION

To illustrate the dependency of the results on the (uncertain) response of potential evapotranspiration to climate change, Fig. 14 shows results obtained using method *L* (no change in mean PET), and *H* (twice the response of the reference M) for constructing future PET. One striking result is that the response of RhineFlow to the different assumptions for PET is relatively constant throughout the year, ranging from 300–400 $m^3 s^{-1}$ in late winter to 400–500 $m^3 s^{-1}$ in summer and autumn. This is caused not only by the direct response of the hydrological model to PET but it is also influenced by the longer, seasonal timescales of soil moisture and groundwater storage. The difference in mean runoff between the standard procedure *M* and one of the two extremes (*L* or *H*) is, in summer, comparable to the difference between the delta and direct approach.

The extreme discharges in Fig. 14 are not very dependent on the assumptions in the estimates of PET, given the large uncertainty band spanned by the *L* and *H* methods. The differences in predicted extremes amount to 300–400 $m^3 s^{-1}$ and the slope of the Gumbel fit is almost identical for both methods. The unrealistically high climate response of PET

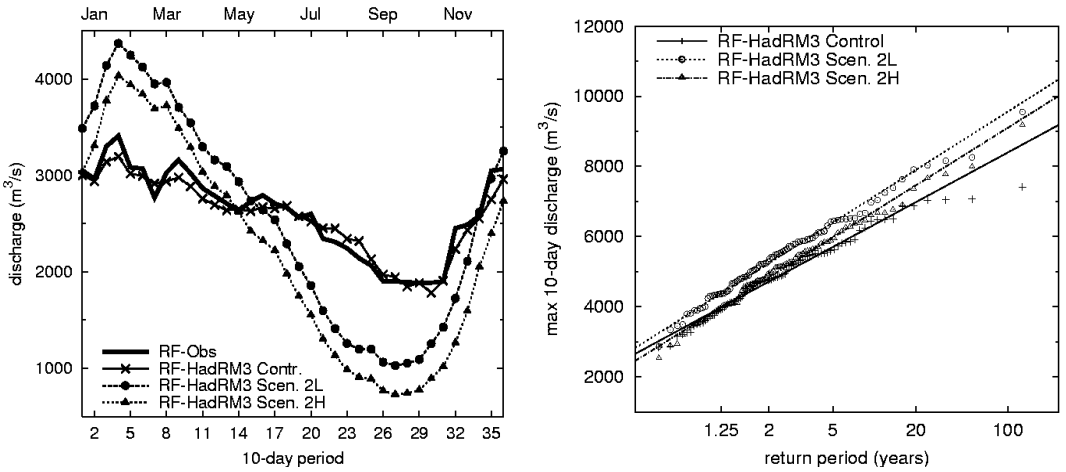

Fig. 14. *The sensitivity of the mean and extreme discharge to the change in PET in the direct model approach, with L denoting no change in mean PET, and H a response twice the response in the standard model simulation (similar to Figs. 12, 13)*

as obtained directly from the model output using the Penman-Monteith equation (more than double the response of scenario H as shown in Fig. 10) had a significant impact on the mean flow and the extremes due to the occurrence of very dry conditions in early winter (not shown).

For all evapotranspiration scenarios, the mean discharge falls below 1000 $m^3 s^{-1}$ in late summer and autumn. Thus, evapotranspiration is not the main cause of the low discharges in summer and the decrease in flow is due mainly to the marked drop in summer rainfall which, in the future simulation, decreases by 50% of the control simulation (Fig. 10).

Bootstrapping

The accuracy of the estimated change of an extreme quantile depends on sample size. A larger sample of annual maximum flows leads to more accurate estimates of the parameters ξ and α of the underlying Gumbel distribution and reduces the uncertainty in the change in the quantiles of the distribution in the future climate. The bootstrap is a simple re-sampling technique to demonstrate this uncertainty.

In the case of the delta approach (scenario 1), the weather of the future climate is connected to that of the present-day climate. In fact, the temperature and precipitation in the future climate resulting from the linear transformation rules given by Eqn. (4) are perfectly correlated with the precipitation and temperature in the control run. Hence, the annual maximum flows in the future and control climate will generally be correlated positively, which may result in a more accurate estimate of the difference between the quantiles of their distribution than in the situation when these annual maximum flows are independent, as is the case with the direct use of the climate model output (scenario 2). The bootstrap is capable of handling both the situation of dependent and independent annual maximum flows.

The following bootstrap technique was used. From the 90 years simulation, J^* years were drawn with replacement for both the control and future climate. To investigate the influence of dependence between the annual maximum flows in the future and control climate, paired bootstrap samples were drawn from the annual maxima in the control and future climates (taking corresponding years out of the 90 years simulation) and also independent samples from the control and future climates. For both paired and independent samples, the change of the 100-year event was estimated by fitting a Gumbel distribution to the annual maximum flows for the control and the future climates and taking the difference between these two estimates. The whole procedure was repeated $B = 20\,000$ times to obtain a frequency distribution of possible predicted changes in the 100-year event. This bootstrap experiment was done for both the annual maximum flows from the HadRM3H scenario 1 and those from the HadRM3H scenario 2.

The results of these experiments are shown in Fig. 15. The direct forcing approach (scenario 2) gives a mean increase of about 900 $m^3 s^{-1}$, consistent with the Gumbel plot in Fig. 13, and a wide band of uncertainty. For the 90-years' sample, the uncertainty is much smaller than that for the 30-years' sample. Though the 100-year event increases in most bootstrap samples, there is a significant probability of predicting a decrease, in particular with the smaller sample size. For the 30-years' sample, this probability is 21%, whereas it decreases to 8% for the 90 years' sample. The

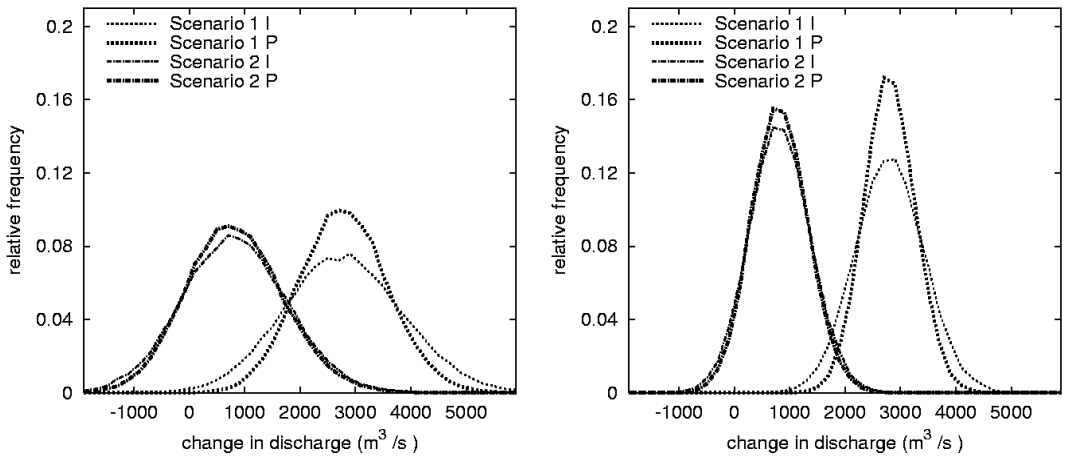

Fig. 15. *Frequency distributions of 20,000 bootstrap replications of the changes in the 100-year flood from the HadRM3H scenario 1 (delta approach) and the HadRM3H scenario 2 (direct model output). Results are shown for bootstrap samples of 30 years (left panel) and 90 years (right panel). P indicates that paired annual maxima from the control and future climate were sampled, and I denotes that the bootstrap samples for the two climates are independent.*

results of independent and paired resampling are similar, because the annual maximum flows in corresponding years of the control and future climate are basically independent. The resampling of the data from the delta approach (scenario 1) leads to a mean increase of 2800 $m^3 s^{-1}$. The result of the paired re-sampling method is somewhat more peaked, but the difference with the independent re-sampling method is not very large. For the direct forcing scenario, the standard errors of the increase in the 100-year flow are about 900 $m^3 s^{-1}$ with 30 years and 500 $m^3 s^{-1}$ with the 90-years-sample size. For the delta scenario these numbers are 800–1100 $m^3 s^{-1}$ for 30 years and 500–650 $m^3 s^{-1}$ for the 90-years sample size (with the smaller numbers based on paired resampling, and the larger numbers based on independent pairs). Thus, the correlation between control climate and future climate in the delta approach does not result in a strong correlation in the extreme discharges. Therefore, the reduction in the uncertainty in the change of the 100-year event due to dependence between the annual maximum flows in the future and control climates in the delta approach might be unimportant from a practical point of view.

Note that the bootstrap technique used here accounts only for the uncertainty because of the limited sample size and not for the uncertainty in the underlying distribution and the differences between climate scenarios. That at least the latter plays a crucial role is evident from the large differences in predicted increase between the direct and the delta approach. Also, extrapolation by fitting a Gumbel distribution might be questioned. The method was chosen here because the discharges observed are well described by a Gumbel distribution, but the discharges simulated appear to deviate from it, in particular in the case of the extremes (c.f. the results for the delta approach). In that case, a GEV distribution might have been a better choice. However, in particular with simulations as short as 30 years, the introduction of one parameter additional to the Gumbel distribution leads to larger error bands at long return periods.

Summary and discussion

Simulations with the hydrological model RhineFlow, driven by data of the HadRM3H regional climate model, for the present and future climates are discussed. To obtain realistic discharges in the present climate, bias corrections to precipitation, temperature and potential evapotranspiration (PET) are necessary. Furthermore, values of PET estimated from HadRM3H using the Penman-Monteith equation are unrealistically high in warm summer months, so a re-construction of PET based on temperature is used (Ekström *et al.,* 2007).

Two methods are employed to construct the future scenarios: scenario 1 is a delta approach based on perturbing the control simulation with mean changes in temperature and precipitation, and scenario 2 is a direct forcing approach correcting the future time series for the biases in the control simulation. Note that for the delta approach, the control climate simulation was perturbed, rather than the observations, which is not the usual application of the delta change approach.

The mean discharge in both scenarios for the future climate increases by about 30% in winter and decreases by about 40% in summer. The delta approach is slightly drier in summer. In winter, differences in the mean are negligible, but the differences predicted in the extremes are

considerable. Extremes were estimated by fitting a Gumbel distribution to the annual maximum discharges. The direct forcing approach predicts an increase of 10% for extreme events with a return period of 100 years, whereas the delta approach predicts an increase of 30%. The predicted extremes appear to be predominantly related to the distribution of precipitation.

The large response of the summer discharge is highly uncertain. It is caused mainly by the large decrease in summer precipitation, of 1.5 mm day^{-1} in the HadRM3H simulations. Seven different RCM simulations driven by the same HadAM3H lateral boundary forcing as in the PRUDENCE project (Christensen *et al.,* 2002), were compared by Van den Hurk *et al.* (2004); most RCMs showed a decrease of only 0.5–0.8 mm day^{-1} in mean summer precipitation for the Rhine basin. The apparent need for additional corrections to the PET computed from the HadRM3H model output using the Penman-Monteith equation raises additional concerns about the applicability of the HadRM3H model data, although the corresponding data of the other RCMs have not been analysed.

The predicted changes in the extreme discharges are very sensitive to the method of scenario production. In Shabalova *et al.* (2003), the results obtained with two different delta approaches, one in which the change in the variance is taken into account and one in which it is ignored, differed significantly (15% in predicted extremes with a return period of 20 years). In addition, the predictability of the change in extreme runoff is limited by the relatively small number of years simulated. Results (obtained with the bootstrap) based on 30 years (out of the total 90 years) show a wide uncertainty band both for the direct and the delta approach (Fig. 15). These results confirm that such extreme events should not be based on simulations of 30 years only, which is at present typical for RCM simulations (cf. Frei and Schär, 2001).

Both direct forcing and delta change scenarios have their pros and cons. On the one hand, the delta approach is transparent in the sense that it places future flows in the context of the historical record, answering questions like: What would the discharges in year X be if the intensity of the precipitation increases by Y percent (Snover *et al.,* 2003). However, it is unclear to what extent climate change can be described by a simple change in the historical time series. How to transfer changes in the frequency of circulation patterns, which may be connected with climate change, into a delta change, is far from trivial. Yet, floods are strongly tied to (the persistency of certain) circulation types (Jacobeit *et al.,* 2003) and there are indications that the recent increase in the number of floods is related to the increase in the frequency of certain critical circulation patterns (Caspary, 1995). On the other hand, the direct approach is capable of representing such complex changes in the climate. However, the direct model output may contain various types of errors, e.g. resulting from RCM errors and imperfect boundaries. This may affect the quality of the discharges in the control climate, even after correction for systematic errors in the means of the variables simulated (Hay *et al.,* 2002). In addition, with each level of correction to the model output, uncertainty is added to the predictions of the discharge.

Finally, the direct and the delta approach are both plausible methods to produce scenarios for the future climate. Both scenarios give the same response in the mean discharge but differ significantly in their extreme values. The delta approach connects better to the (observed) variability in the present-day climate, whereas the direct approach may be more successful in coping with complex changes, which is an advantage when considering extreme events. However, only a rather simple form of the delta approach has been tested whereas, with more complex transformation rules, better results might result from the delta approach. Model development will continue to lead to improved model representations of the climate system, thereby reducing the need for bias corrections. Hence, the direct forcing approach, despite its present limitations in simulating the (present-day) climate, has the better future prospects.

Acknowledgments

The HadRM3H data were supplied by the Climate Impacts LINK project, DEFRA Contract EPG 1/1/124, on behalf of the Hadley Center and UK Met Office. The meteorological data were made available by the following institutions: Deutscher Wetterdienst, Service de la météorologie et de l'hydrologie de Luxembourg, Météo France and Swiss Meteorological Institute, via the International Commission for the Hydrology of the Rhine basin (CHR/KHR). This research was supported, in part, by the EU Energy, Environment and Sustainable Development programme (contract: EVK1-CT-2000-00075, SWURVE). The Institute for Inland Water Management and Waste Water Treatment (RIZA) is thanked for its contribution to SWURVE.

References:

Brandsma, T., 1995. *Hydrological impact of climate change, a sensitivity study for the Netherlands*. PhD thesis, Delft University of Technology.

Caspary, H.J., 1995. Recent winter floods in Germany caused by changes in the atmospheric circulation across Europe. *Phys. Chem. Earth*, **20**, 459–462.

CHR, 1976. *Le Basin du Rhin. Monographie Hydrologique*. Commission internationale de l'hydrologie du basin du Rhine, the Hague, The Netherlands.

Christensen, J.H., Carter, T.R. and Giorgi, F., 2002. PRUDENCE employs new methods to assess European climate change. *EOS*, AGU, **82**, 147.

Ekström, M., Jones, P.D., Fowler, H.J., Lenderink, G., Buishand, T.A. and Conway, D., 2007. Regional climate model data used within the SWURVE project 1: projected changes in seasonal patterns and estimation of PET. *Hydrol.Earth Syst. Sci*, **11,** 1069–1083.

Frei, C. and Schär, C., 2001. Detection probability of trends in rare events: Theory and application to heavy precipitation in the Alpine region. *J. Climate*, **14**, 1564–1584.

Frei, C., Christensen, J.H., Déqué, M., Jacob, D., Jones, R.G. and Vidale, P.L., 2003. Daily precipitation statistics in regional climate models: Evaluation and intercomparison for the European Alps. *J. Geophys. Res*., **108 (D3)**, 4124, doi:10.1029/2002JD002287.

Giorgi, F., Bi, X. and Pal, J., 2004. Means, trends and interannual variability in a regional climate change experiment over Europe. Part I: Present-day climate (1961-1990). *Clim. Dynam*., **22**, 733–756.

Graham, L.P., 2004. Climate change effects on river flow to the Baltic Sea. *Ambio* (In press).

Hagemann, S., Machenhauer, B., Christensen, O.B., Déqué, M., Jacob, D., Jones, R.G. and Vidale, P.L., 2004. Evaluation of water and energy budgets in regional climate models applied over Europe. *Clim. Dynam*., **23**, 547–567.

Hay, L.E., Wilby R.L. and Leavesley, G.H., 2000. A comparison of delta change and downscaling GCM scenarios for three mountainous basins in the United States. *J. Amer. Water Resour. Assoc.,* **36**, 387–398.

Hay, L.E., Clark, M.P., Wilby, R.L, Gutowski, W.J., Leavesley, G. H., Pan, Z., Arritt, R.W. and Takle, E.S., 2002. Use of regional climate model output for hydrologic simulations. *J. Hydrometeorol.,* **3**, 571–590.

Jacobeit, J., Glaser, R., Luterbacher, J. and Wanner, H., 2003. Links between flood events in central Europe since AD 1500 and large-scale atmospheric circulation modes. *Geophys. Res. Lett*., **30**, 1172, doi:10.1029/2002GL016433.

Johns, T.C., 2003. Anthropogenic climate change for 1860 to 2100 simulated with the HadCM3 model under updated emission scenarios. *Clim. Dynam.,* **20**, 583–612.

Jones, R., Murphy, J., Hassell, D. and Taylor, R., 2001. *Ensemble mean changes in a simulation of the European climate of 2071-2100 using the new Hadley Centre regional modelling system HadAM3H/HadRM3H.* Hadley Centre Report, Met Office Bracknell, UK.

Jones, C.G., Willén, U., Ullerstig, A. and Hansson, U., 2004. The Rossby Centre Regional Atmosphere Model Part I: Model climatology and performance for the present climate over Europe. *Ambio,* **33**, 211–220.

Klein Tank, A,M.G. and Können, G.P., 2003. Trends in indices of daily temperature and precipitation extremes in Europe, 1946-99. *J. Climate,* **16**, 3665–3680.

Kwadijk, J. and Rotmans, J., 1995. The impact of climate change on the discharge of the river Rhine: a scenario study. *Climatic Change*, **30**, 397–426.

Middelkoop, H. (Ed.), 2000. *The impact of climate change on the river Rhine and the implications for water management in the Netherlands*. Summary report of the NRP project 952210. RIZA Report 2000.010, RIZA, Lelystad, The Netherlands.

Nakicenovic, N., Alcamo, J., Davis, G., de Vries, B., Fenhann, J., Gaffin, S., Gregory, K., Grübler, A., Jung, T.Y., Kram, T., La Rovere, E.L., Michaelis, L., Mori, S., Morita, T., Pepper, W., Pitcher, H., Price, L., Riahi, K., Roehrl, A., Rogner, H.-H., Sankovski, A., Schlesinger, M., Shukla, P., Smith, S., Swart, R., van Rooijen, S., Victor, N. and Dadi, Z., 2000. *IPCC Special Report on Emissions Scenarios*. Cambridge University Press, Cambridge, UK. 599 pp.

Räisänen, J., Hansson, U., Ullerstig, A., Döscher, R., Graham, L.P., Jones, C., Meier, H.E.M., Samuelsson, P. and Willén, U., 2004. European climate in the late twenty-first century: regional simulations with two driving global models and two forcing scenarios. *Clim. Dynam*., **22**, 13–31.

Shabalova, M.V., van Deursen, W.P.A. and Buishand, T.A., 2003. Assessing future discharge of the river Rhine using regional climate model integrations and a hydrological model. *Climate Res*., **23**, 233–246.

Snover, A.K., Hamlet, A.F. and Lettenmaier, D. P. 2003. Climate-change scenarios for water planning studies: pilot applications in the Pacific Northwest. *Bull. Amer. Meteorol. Soc*., **84**, 1513–1518.

Tackle, E.S. *et al*., 1999. Project to Intercompare Regional Climate Simulations (PIRCS): description and initial results. *J. Geophys. Res.,* **104**, 1443–1461.

Thornthwaite, C.W. and Mather, J.R., 1957. Instructions and tables for computing potential evapotranspiration and the water balance. In: *Publications and climatology. Vol. 10*. Laboratory of Climatology, Drexel Institute of Technology, Centerton, NJ, USA. 183–243.

Van den Hurk, B., Hirschi, M., Schär, C., Lenderink, G., van Meijgaard, E., van Ulden, A., Rockel, B., Hagemann, S., Graham, P., Kjellström, E. and Jones, R., 2005. Soil control on runoff response to climate change in regional climate model simulations. *J. Climate,* **18**, 3536–3551.

Van Deursen, W.P.A. and Kwadijk J., 1993. RHINEFLOW: an integrated GIS water balance model for the river Rhine. In: *Application of Geographic Information Systems in hydrology and water resources management*, K. Kovar and H.P. Nachtnebel (Eds.), *IAHS publication no. 211*, 507–519.

Vidale, P.L., Lüthi, D., Frei, C., Seneviratne, S. and Schär, C., 2003. Predictability and uncertainty in a regional climate model. *J. Geophys. Res*., **108(D18)**, 4586, doi: 10.1029/2002JD002810.